Geotech Geol Eng (2020) 38:1919–1938
https://doi.org/10.1007/s10706-019-01139-x

ORIGINAL PAPER

Horizontal and Vertical Geotechnical Variations of Soils According to USCS Classification for the City of An-Najaf, Iraq Using GIS

Sohaib Kareem Al-Mamoori · Laheab A. Jasem Al-Maliki · Ahmed H. Al-Sulttani · Khaled El-Tawil · Hussain M. Hussain · Nadhir Al-Ansari

Received: 16 April 2019 / Accepted: 7 December 2019 / Published online: 13 December 2019

Abstract The unified soil classification system (USCS) first proposed by Casagrande and subsequently developed by the Army Corps of Engineers. It widely used in many building codes and books. An-Najaf city is the most important city in Iraq due to its religious and spiritual value in the Muslim world, so it is fast expanding and continuous developing city in Iraq. The data from 464 boreholes in the study area for depths of 0–26 m have been used. 13 Soil samples were collected from each borehole with 13 depths level (0–26) m with 2 m intervals. The USCS was applied to the soil samples from 13 depth levels borehole. This research aims to create a geodatabase for soil properties for An-Najaf. The ArcGIS 10.5 software was used to interpolate the spatial data to produce 33 geotechnical maps for fine soil, coarse soil and USCS for 13 depth levels. For numerical soil data, Ordinary Kriging has been used for interpolation mapping of Fine and Coarse percentage data for each depth. For non-numerical (nominal) soil data (USCS class), the Indicator Kriging method is used. The results show that the coarse soil occupied 85–95% for depth 0–16 m and consist of (SP, SP-SM, SM) while fine soil occupied 5–15% consisting of (OL, CH, ML) subsequently, this soil when compacted has a permeability of pervious to semi impervious, good shearing strength, low to very low compressibility and acceptable workability as a construction material. The results also show that after 16 m depths until 26 m, the fine soil percentage increased to 40% with a coarse soil

S. K. Al-Mamoori · A. H. Al-Sulttani
Department of Environmental Planning, Faculty of Physical Planning, University of Kufa, Najaf, Iraq
e-mail: sohaib.almamoori@uokufa.edu.iq

A. H. Al-Sulttani
e-mail: ahmedh.alsulttani@uokufa.edu.iq

L. A. Jasem Al-Maliki
Department of Hydraulic Engineering Structures, Faculty of Water Resources Engineering, University of Al-Qasim Green, Babylon, Iraq
e-mail: laheab.almaliki@wrec.uoqasim.edu.iq

K. El-Tawil
Faculty of Engineering, Lebanese University, Beirut, Lebanon
e-mail: khaled_tawil@ul.edu.lb

H. M. Hussain
Department of Geology, Faculty of Science, University of Kufa, Najaf, Iraq
e-mail: hussainm.alshimmary@uokufa.edu.iq

H. M. Hussain
Remote Sensing Center, University of Kufa, Najaf, Iraq

N. Al-Ansari (✉)
Department of Civil, Environmental and Natural Resources Engineering, Lulea University of Technology, Luleå, Sweden
e-mail: nadhir.alansari@ltu.se

percentage of 60%, indicating changes in soil characteristics as the permeability became semi-pervious to impervious, fair shearing strength, medium compressibility and fair workability as a construction material. The study results will provide help and saving time, efforts and money in preliminary engineering designs.

Keywords Geotechnical · USCS · Soil types · GIS · Kriging · Najaf

1 Introduction

Classifying soil is a way to arrange it into groups or subgroups to describe its characteristics concisely (Das 2013) (Das and Sobhan 2013; Das 2013). It is essential to clarify the soil classes before designing and constructing any project as the engineering characteristics of soil (stiffness, permeability, and strength) are influenced by the soil particles' shape, size, arrangement and microscopic structure (Budhu 2015).

Generally, soils are classified into (fine-grained) or (granular or coarse-grained) soils depending on the distributions of particles of the same size. Fine soils are determined by the percentage of the soil mass passing through a 0.075 mm sieve, while granular soils are the soil mass that retained in a 0.075 mm sieve, including sand, gravel, cobbles, and boulders. If the percentage of fine soil passes through the sieve at a predefined proportion, usually 50% (but this could be less according to the soil classification system used), the soil is considered as Fine-grained. Fine-grained soils are furthermore classified into clay or silt using a hydrometer test. Finally, soils are subclassified according to their consistency (Reale et al. 2018).

There are many soil classification systems used by engineers, and they mostly use the same criteria for classification, such as the distribution of particles and plasticity (Das and Sobhan 2013). However, the two main systems used by engineers are the unified system and the AASHTO system, and they are both almost similar in using simple index properties like grain-size and Atterberg limits (Das and Sobhan 2013; ASTM 2000).

Sundry studies have conducted regarding the geotechnical properties of soil in different Iraqi regions. Al-Baghdadi (2016) prepared a set of maps for An-Najaf city using the (SURFER 11) software to produce a contour line for different geotechnical properties of the soil (Al-Baghdadi 2016). Ali and Fakhraldin (2016) investigated and analysed the physical and chemical soil properties of five selected locations for An-Najaf city (Ali and Fakhraldin 2016). Al-Shakerchy and Al-Khuzaie (2011) introduced geotechnical maps of the Iraqi governorates of Baghdad, Diyala, Wasit, and Babylon using the (SURFER 7) software. Al-Maliki et al. (2018) produced a GIS map for the soil allowable bearing capacity of AN-Najaf city at depths 0–2 m (Al-Maliki et al. 2018). Al-Mamoori and his colleagues conducted studies for different geotechnical soil properties to build a geodatabase for the city of AN-Najaf, which will be helpful in the preliminary design stage (Al-Mamoori 2017; Al-Mamoori et al. 2018, 2019). Geographic information systems (GIS) are widely used for spatial data handling and manipulation. A geotechnical assessment usually requires a large amount of spatial data. It is a robust and useful tool for analyzing large quantities of data for geotechnical assessments and the undertaking of similar analyses on very large areas in a short period of time. A paramount feature of the GIS is its capability to create new data by combining current varied data that share a compatible spatial referencing system (Dai et al. 2001).

This paper is part of a series of research papers aiming to create an extensive geodatabase for soil chemical and physical properties for part of the Najaf governorate using GIS. The objective of this paper is to produce the geotechnical maps for the unified soil classification system of the study area and assess the geotechnical suitability of the foundations of residential areas. A GIS (ArcMap 10.5) software was used. For determining the geotechnical properties of the study area, data from 464 boreholes were used.

2 Study Area Description

An-Najaf city is a double city (An-Najaf and Kufa) and is considered the capital of An-Najaf province, which is one of the eighteen provinces of Iraq. The city is situated 161 km to the southwest of the Iraqi capital, Baghdad on the edge of Mesopotamia (Tigris and Euphrates flood plain) in the east of the city, and of the southern desert (Western Plateau) in the west, and the

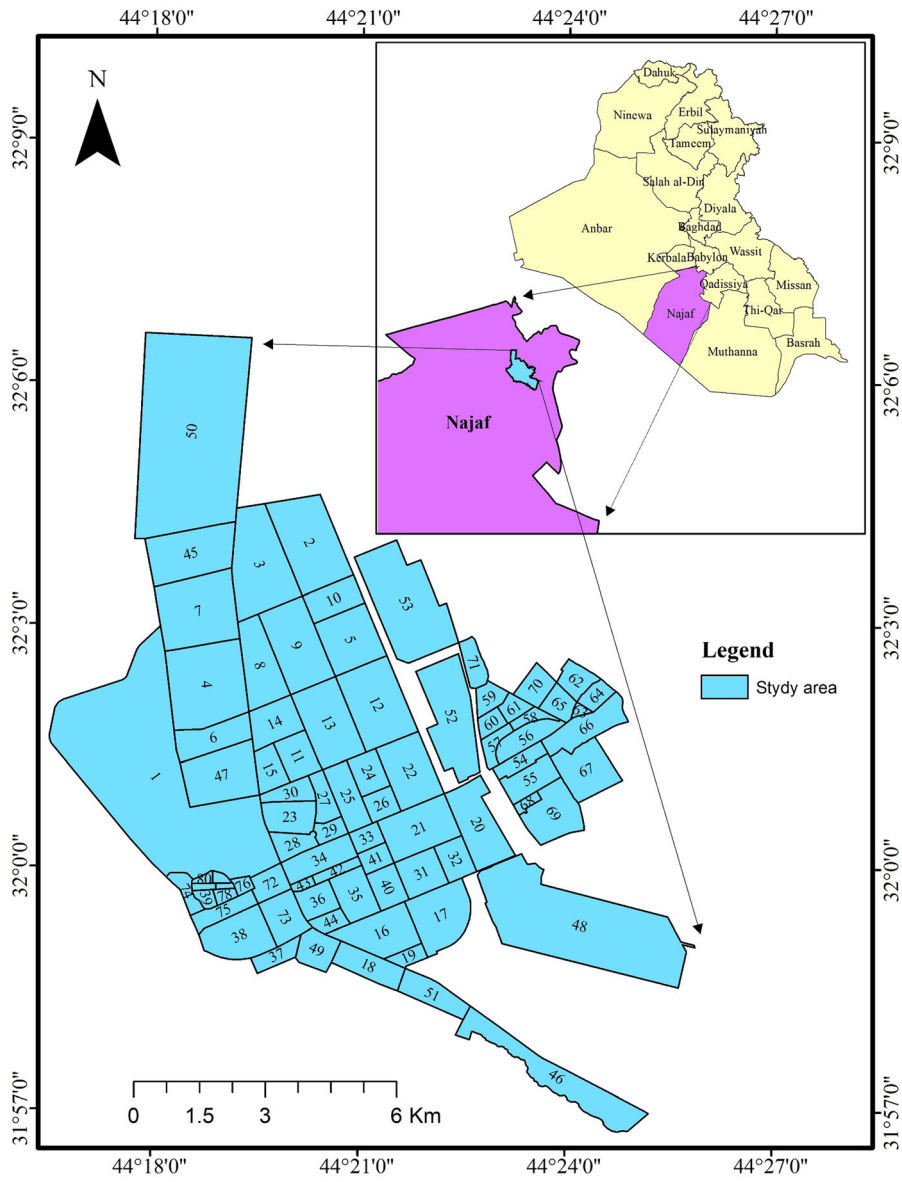

Fig. 1 Study area location

ground slopes gently toward the flood plain (Al-Mamoori et al. 2019).

An-Najaf and Kufa city are situated between 44° 17′ 00″ and 44° 25′ 0″ East and 32° 7′ 0″ and 31° 56′ 0″ latitudes North (Fig. 1). This area is considered one of the most continuously developing urban areas, and it currently covers an area of approximately 105.1 km^2. Each neighborhood in the selected study area has been given a corresponding number, as displayed in Table 1.

The climate of An-Najaf city is characterized as an arid and semi-arid, with long hot and dry summers with an average temperature of about 45 °C, and short winters with an average temperature of 24 °C. The rainy season runs from October to April. The average gross annual rainfall is about 100 mm in a wet year, and about 30 mm in a dry year (Mail et al. 2016; Beg and Al-Sulttani 2020).

For soil characteristics of the study area, the internal friction angle Ø of An-Najaf soil varies

Table 1 Neighborhood numbering. *Source*: after (Al-Mamoori et al. 2019)

No.	Neighbourhood	No.	Neighbourhood	No.	Neighbourhood
1	Wadi Al-Salam	28	Al Hannana	55	Maytham Al Tammar
2	Al-Askari	29	Al Sahha	56	Kinda1
3	Al Makrama	30	Al Ulama'a & Al Shuara'a	57	Al Shurta
4	Al Nasr	31	Al Zahra'a	58	Al Mua'alimeen
5	Al Wafa'a	32	Al Qadissiea	59	Al-Askari
6	Abu Talib	6 + 33	Al Askan	60	Al Mutanabbi
7	Al Meelad	34	Al Sa'ad	61	Al Jamia'a
8	Al Jam'iea	35	Adan	62	Al Jedaydat
9	Al Urooba	36	Al Mua'alimeen	63	Al Waqf
10	Al Indiea	37	Al Shurta	64	Al Rashadiea
11	Al Ghari	38	Al Jidayda 4	65	Al Jamhooriea
12	Al Jami'aa	39	Al Hwoaysh	66	Al Safeer
13	Al Salam	40	Al Hawra'a	67	Al Furat
14	Al Salam Al jadeed	41	Al Eshtiraki	68	Door Al Ma'amal
15	Al Atibba'a	42	Al Muthanna	69	Al Sadr Al Thalith
16	Al Ansar	43	Abu Khalid	70	Al Suhayliea
17	Al Harafieen	44	Al Mahdi	71	Al Sahla
18	Al Quds2	45	Al Meelad Al Jadeed	72	Al Jidayda 1
19	Al Quds1	46	Al Randhawa	73	Al Jidayda 3
20	Al Sina'ei	47	Al Rahma	74	Tourism Zone
21	Al Ameer	48	Najaf National Airport	75	Al Jidayda 2
22	Al Adala	49	Scientific City	76	Commercial Zone
23	Al Hussien	50	Al Nida'a	77	Imam Ali Shrine
24	Al Furat	51	Najaf Technical Institute	78	Al Buraq
25	Al Ghadeer	52	Kufa University	79	Al Mishraq
26	Civil Offices	53	Meesan	80	Al Emara
27	Al Karama	54	Kinda2	81	Al Sooq Al Kabeer

between 26.3 and 41.2 in most of the region (Ali and Fakhraldin 2016). The bearing capacity ranges between 5 and 20 Ton/m^2 in this region (Al-Maliki et al. 2018). While the percentage of sulfate content ranges between 0.36 and 14% for soil and varies between 84 and 239% in groundwater (Al-Mamoori et al. 2018). The gypsum content ranges between 10 and 25%, values that are considered very high (Al-Mamoori 2017). The liquid limit (LL) and plastic limit (PL) vary from 21 to 29% and 11 to 15%, respectively. The low values of LL and PL for the soil in western locations increases towards the eastern locations. The maximum dry density and optimum moisture content vary from 17 to 19 KN/m^3 and 8 to 14%, respectively (Ali and Fakhraldin 2016).

Geologically, the study area is covered by different deposits. The oldest is the Dibdiba formation (Pliocene–Pleistocene), which is exposed in a small area in the Tar An-Najaf, west of study area. The lithological component of the Dibdiba is sandstone. Ill-sorted, fine-coarse grained small pebbles often reported with a thickness of about 10 m (Barwary and Slewa 1995). The lower contact of the Dibdiba formation is with the Injana Formation (Upper Miocene). The thickness of the Injana ranges from 20 to 35 m, and it is composed mainly of red, partly greenish silty, sandy calcareous clay stone and lenticels of grey, brownish, greenish and yellowish sandstone, and thin beds (0.30 m.) of marly and chalky limestone are occasionally present in the sequence (Buday 1980; Barwary and Slewa 1994). The Dibdiba formation is non-uniformly covered by Gypcrete (Pleistocene–Holocene), which is found in most of the study area to a thickness of (0.5–2) m of secondary

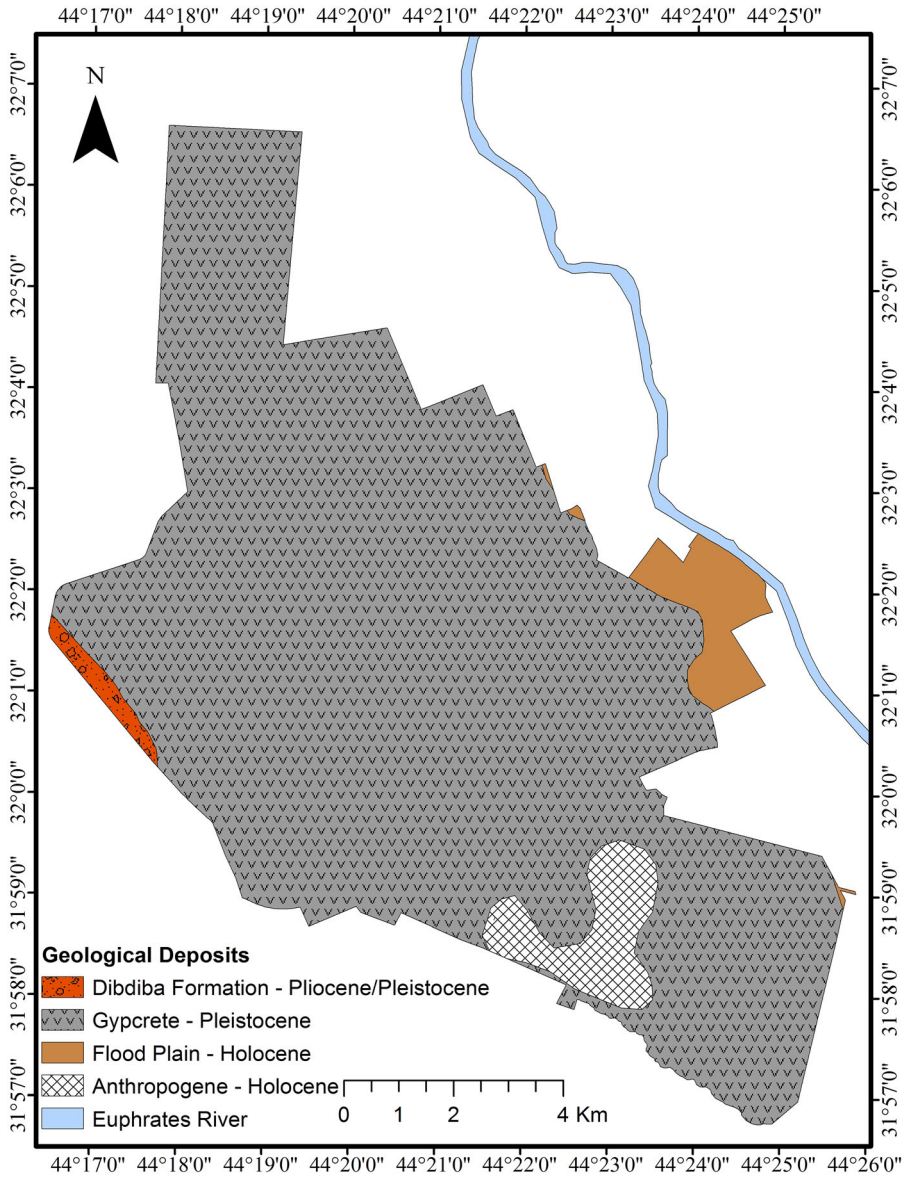

Fig. 2 Geological deposits formation in the study area Source: After (Barwary and Slewa 1994; Barwary and Slewa 1995)

gypsum in a powdery form or fibrous prismatic, hard well-crystallized form, and as brownish spongy form (Al-Mubarak and Amin 1983). The Holocene deposits are Flood plain and Anthropogenic deposits, and these are found in a small area in the east and south of study area. Flood Plain deposits consist of a loam which is a mixture of clayey silt deposits from the Euphrates river to a thickness of up to 15 m (Jassim and Goff 2006). Anthropogenic deposits are mainly composed of the bodies of ancient irrigation canals and hillocks of ancient settlements (Barwary and Slewa 1994) (Fig. 2).

3 Materials and Methods

The study draws on data from 464 boreholes "(Appendix)", with 13 soil tests for each borehole starting at a depth of 0–2 m and increasing to 24–26 m. Two approaches have been utilized to calculate the SPT-N-

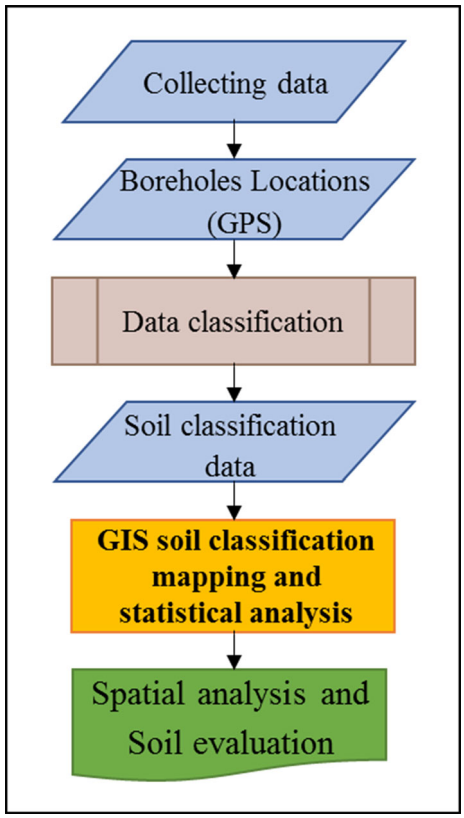

Fig. 3 Flowchart of the work

value. The first approach involved collecting the geotechnical data, and the second data set arranged by using Excel to make it familiar with the ArcGIS 10.5 environment. The coordinates of the spatial boreholes are designated by using the GPS device. The geotechnical maps were created using the ArcGIS 10.5 software, (Fig. 3).

3.1 Materials

The study data obtained from the reports of the National Center for Construction Laboratories & Researches (NCCLR)/Babylon laboratory, which is a branch of the National Center for Construction Laboratories & Research (NCCLR). NCCLR is a branch of the Iraqi Construction and Housing Ministry. Since its establishment in 1977, the laboratory (NCCLR) has been performing soil tests for the Euphrates river basin area (known as the Middle Euphrates region) besides testing construction materials (NCCLR 2016). The data used was collected from 464 boreholes spread throughout An-Najaf and Kufa cities at depths of 0–26 m. Borehole locations are presented in (Fig. 4). The data contain the sieve analysis for boreholes and the plastic and liquid limits among many other soil properties.

3.2 Methods

3.2.1 USCS Classification

The Unified Soil Classification System is first proposed by Casagrande in 1942 and developed in 1952 by the Army Corps of Engineers (Das and Sobhan 2013). It is widely used in many building codes and books (Reale et al. 2018; Robertson 2016). The soil in this classification system is divided into two master divisions: coarse soil (gravel and sand) and fine soil (clay and silt). If the retained soil in a No. 200 sieve is more than 50%, then the soil is coarse but, if the soil passes through a No. 200 sieve, then the soil is fine (Reese et al. 2006). The soil is then further classified by several subdivisions, as shown in Table 2 (Das 2013).

3.2.2 GIS Mapping

A geographic information system (GIS) is a set of rules and tasks for data analysis and processing using a computer. It is used to link information to its geographical location according to the coordinates, to arrange data into layers and then to transform it into maps for the selected area and thus show the geographic or other attributes of that area. As each borehole has its spatial data and geotechnical data, this data has been arranged and horizontally tabulated in the Excel software in a way that is convenient for the ArcGIS 10.5 environment. The interpolation is an estimation of a value within two known values in a sequence of values; in other words, it is a procedure used to predict the values of cells at specific locations that have missing sample data (Childs 2004).

The best approach to soil mapping is by using interpolation techniques, and there are many methods of interpolation. For numerical soil data, for example, the best method for interpolation is Ordinary Kriging (OK) (Bhunia et al. 2018; Zandi et al. 2011), and this method has been used for the interpolation of Fine and Coarse percentages for each depth while for the USCS soil classes, in our case, the classes of USCS are

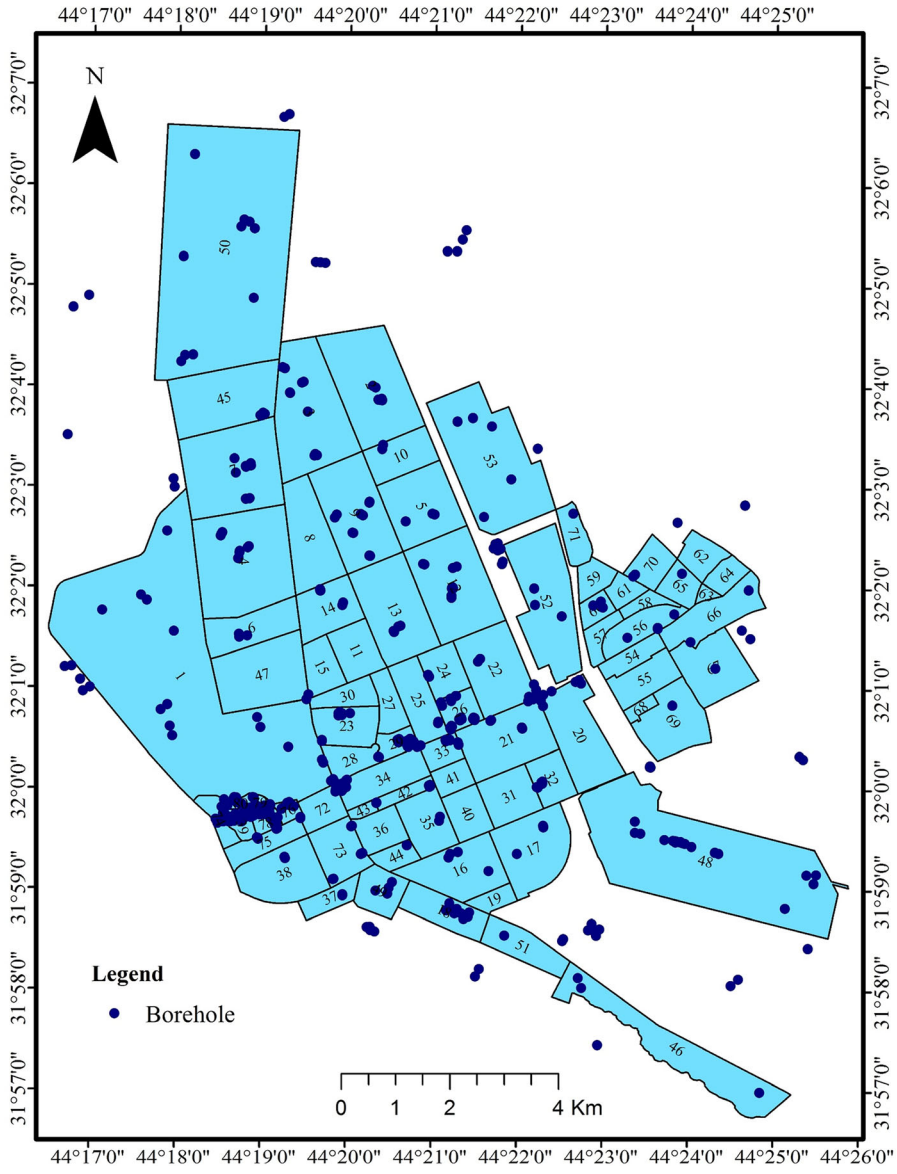

Fig. 4 Borehole locations

categorical data (nominal), the Indicator Kriging (IK) method has been used because it is considered as the best interpolation methods for categorical (nominal) data (Mendes and Lorandi 2006; Liu et al. 2012). All the interpolated maps have produced with cell size (pixel) 20 m.

4 Results and Discussion

This study is the first of its kind in Iraq to apply the Unified Soil Classification System to the soil of the study area to produce geotechnical maps for soil classes and soil types using the ArcGIS software. The data used are from 464 boreholes for depths of up to 26 m. Geotechnical maps for soil classes and soil types produced, as seen in (Figs. 5, 6, and 7):

The results maps show the followings (Figs. 5, 6, and 7):

a. Coarse soils: the classes present are (SP, SP-SM, SM), distributed as shown in the study area, which lacks the classes (Gravels: GW, GP, GM, GC) or (SW, SC), which indicate that the soil is poorly

Table 2 Unified soil classification system classes. *Source*: after (Das 2013; ASTM 2000)

Major divisions	Group symbols (classes)	Typical names
Gravels	GW	Well-graded gravels; gravel-sand mixtures (few or no fines)
	GP	Poorly graded gravels; gravel-sand mixtures (few or no fines)
	GM	Silty gravels; gravel–sand–silt mixtures
	GC	Clayey gravels; gravel–a sand-clay mixture
Sands	SW	Well-graded sands; gravelly sands (few or no fines)
	SP	Poorly graded sands; gravelly sands (few or no fines)
	SM	Silty sands; sand–silt mixtures
	SC	Clayey sands; sand-clay mixtures
Fines	ML	Inorganic silts; very fine sands; rock flour; silty or clayey fine sands
	CL	Inorganic clays (low to medium plasticity); gravelly clays; sandy clays; silty clays; lean clays
	OL	Organic silts; organic silty clays (low plasticity)
Fines Silts and clay (liquid limit greater than 50)	MH	Inorganic silts; micaceous or diatomaceous fine sandy or silty soils; elastic silt
	CH	Inorganic clays (high plasticity); fat clays
	OH	Organic clays (medium to high plasticity); organic silts
Highly organic silts	Pt	Peat; mulch; and other highly organic soils

graded silty sands. The percentage for gravels was less than 15%, so it was not considered.

b. Fine soils: the present classes are (OH, OL, CH, CL, ML), distributed as shown in the study area, that lacks the classes (MH, PT), which indicate that the soil is silty, clay, or mixed organic soils with low or high plasticity.
c. SP soil class distribution is combined with the distribution of SP-SM class almost on all depths. Also, it is noticed, that the distribution area of SP and SP-SM shrinks with depth to the north and east and small area in the middle.
d. SM class is dominant in the study area in all depths and its area increases with depth.
e. ML and CL classes occupy spotted small areas in the middle, east and south and spread with depth to the north of the study area.
f. OL and OH classes mostly are diapered in the first three depths levels (0–6) m, but they have a considerable area with depth. They cover a small area in the southern part at depth (6–8) m and expand with depth in the middle, west and north of the study area.

The Trend linear line and R-square for soil class was drawn and calculated to illustrate the change in the class percentage with depth as follows Table 3, (Fig. 8):

a. Silty Sands (SM): This class comprises the greater percentage of the soil for all depths. Its percentage was 62% at 2 m, and 52% at 26 m. Its percentage is nearly constant with depth (Fig. 8e), which is why its R^2 is approximately 0.00009.
b. Poorly graded sands and silty sand (SP-SM): this soil class occupies the second rank, with a percentage of 39.6% up to a depth of 16 m, after which its values reduce to 6.6%. The (R^2) between the percentage and the depth was 0.826, and the correlation relationship is a strong inverse correlation (see Fig. 8c).
c. Poorly Graded Sands (SP): this class is the third large percentage (62%) in the soil from 0 to 16 m depth. After 16 m, its values begin to reduce with the depth until it reaches 0%. The (R^2) between the percentage and the depth was 0.78, and the correlation relationship is a strong inverse correlation (see Fig. 8a).
d. Silts of Low Plasticity (ML): this class of soil, which describes fine soils, is the fourth rank in percentage until 16 m in depth. After 16 m in-depth, this class comprises the second-largest soil

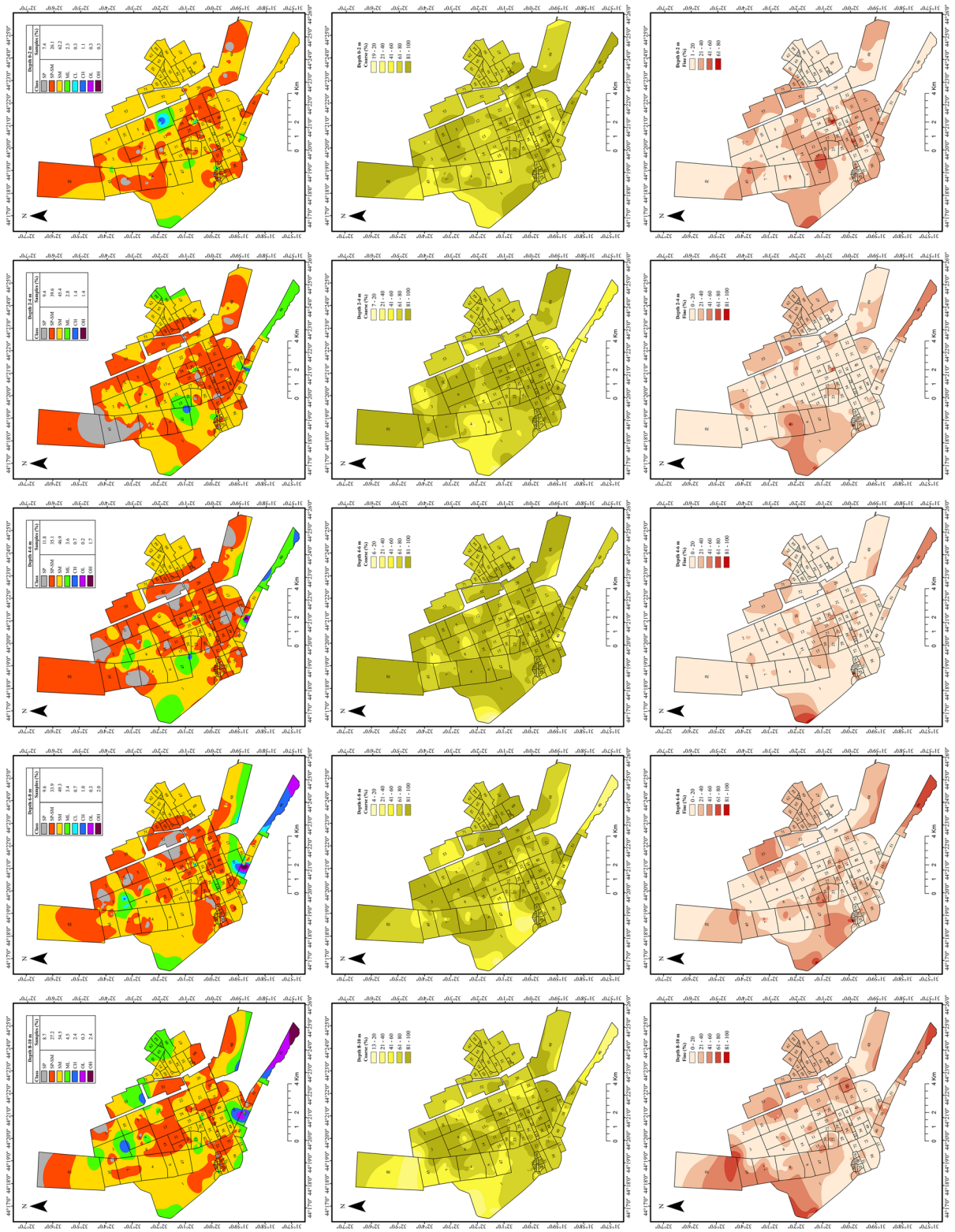

Fig. 5 Geotechnical maps for (USCS), coarse and fine soils percentage for depths (0-10) m

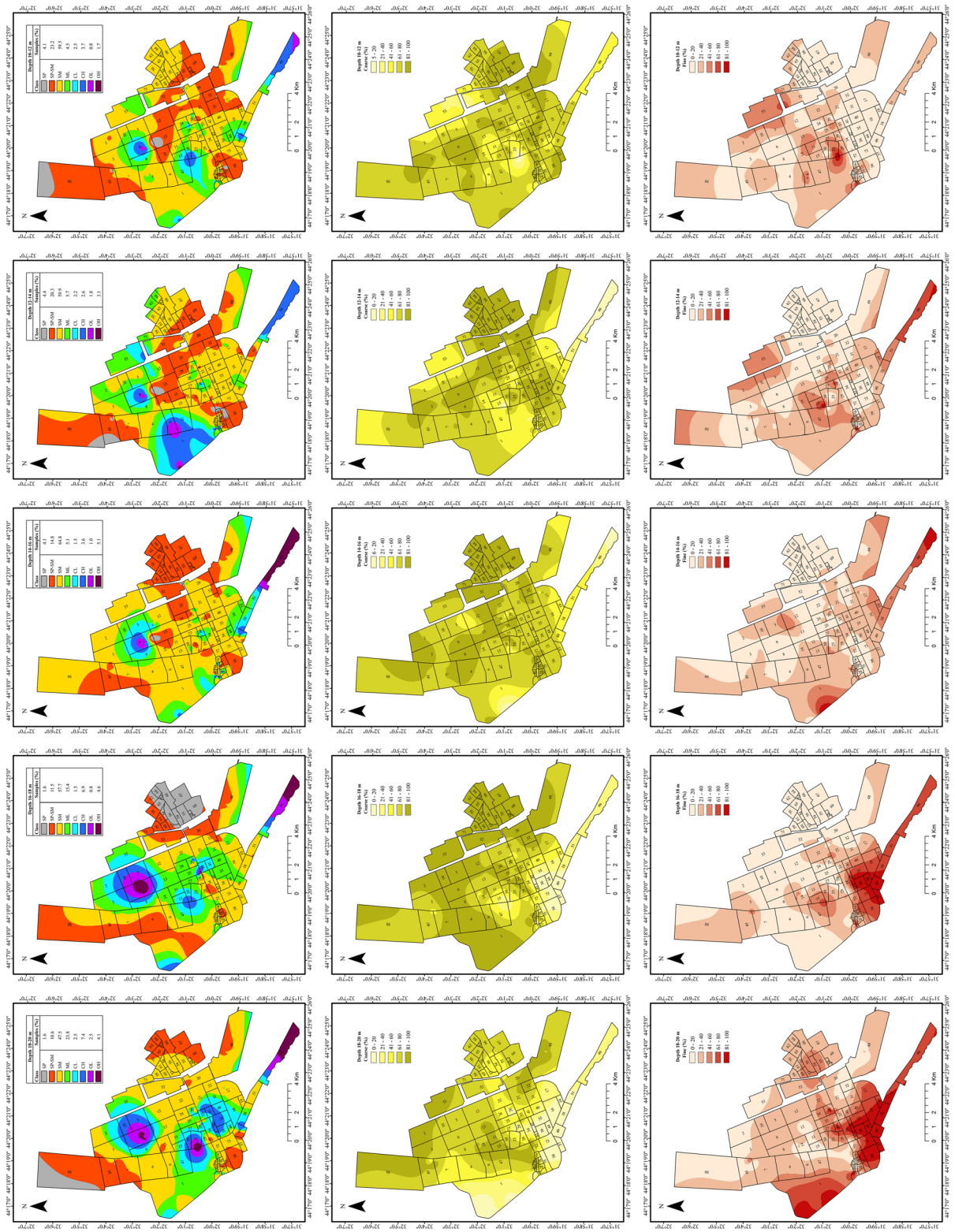

Fig. 6 Geotechnical maps for (USCS), coarse and fine soils percentage for depths (10-20) m

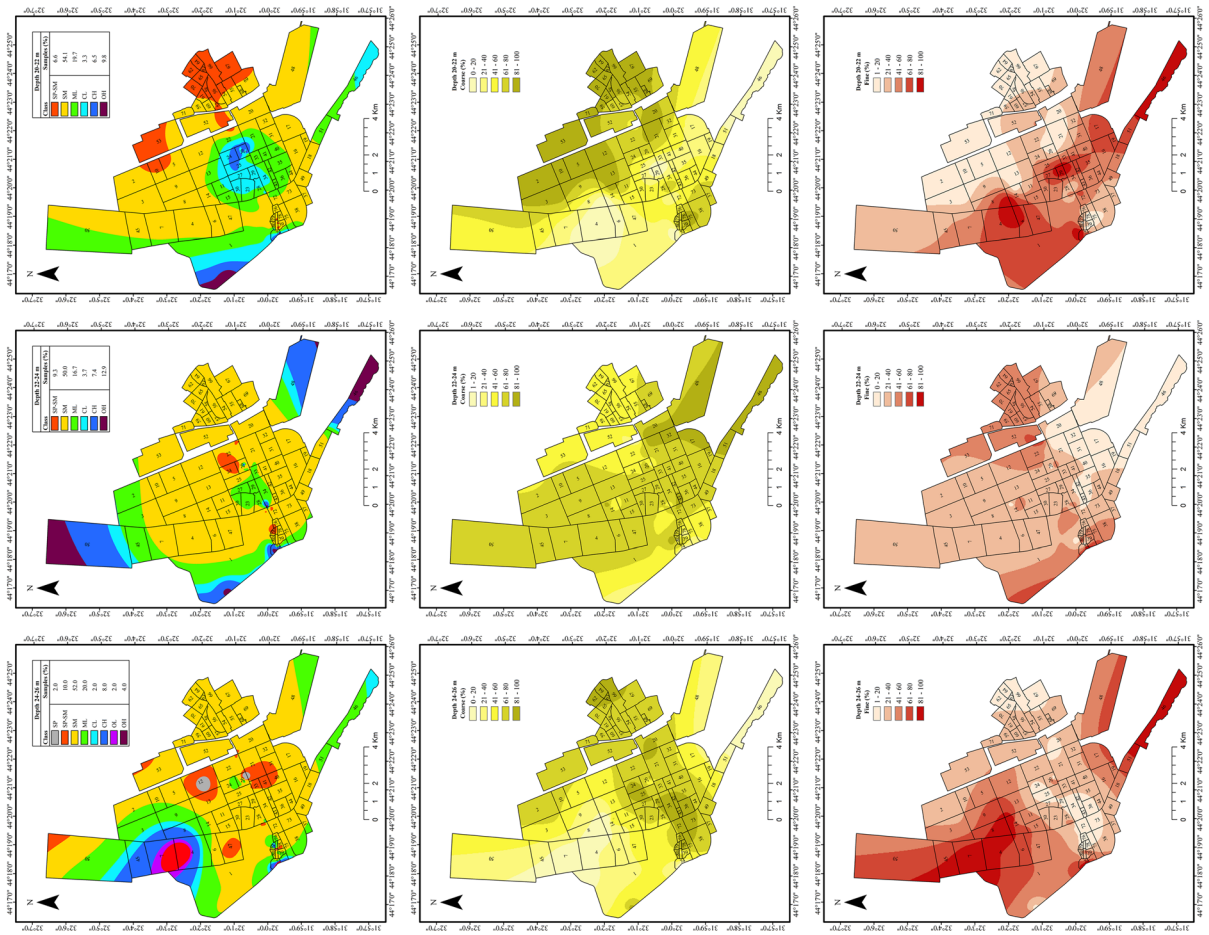

Fig. 7 Geotechnical maps for (USCS), coarse and fine soils percentage for depths (20-26) m

percentage, as its values increase with depth until reaching 20%. The (R^2) between the percentage and the depth was 0.76, and the correlation relationship is a strong extrusive correlation (see Fig. 8g).

e. The clay of Low Plasticity (CL) and Clay of High Plasticity (CH): these classes are present in small percentages for depths of 0–16 m, after increasing depth their values start to increase. The (R^2) between the percentage and the depth for CL and CH was 0.68 and 0.88, respectively. The correlation relationship was a medium extrusive correlation for CL, and a strong extrusive correlation for CH (see Fig. 8b, d).

f. Organic Silt, Clay of High Plasticity (OH) and Organic Silt, Clay of Low Plasticity (OL): these classes of fine soil were present in the study area at a very small percentage (OH = 0.3% and OL = 0%) until a depth of 16 m. After this depth, their percentages increase to reach (OL = 2.5 & OL = 12.9). The (R2) between the percentage and the depth was 0.19 for OL, and 0.57 for OL. See (Fig. 8f, h).

In Fig. 9, each class has drawn against its percentage in two depths ranges: first, from 0 to 16 m and, second, from 16 to 26 m. This is done to analysis the change in the soil types before and after the 16 m depth. The figure show that the coarse soil classes (SP,

Table 3 Percentage of soil classes with depths

Soil classes	R^2	(0–2) m	(2–4) m	(4–6) m	(6–8) m	(8–10) m	(10–12) m	(12–14) m	(14–16) m	(16–18) m	(18–20) m	(20–22) m	(22–24) m	(24–26) m
SP	0.7841	7.4	9.4	11.8	9.6	8.7	4.1	4.4	4.1	1.6	1.6	0.0	0.0	2.0
SP-SM	0.8261	26.1	39.6	35.1	33.8	27.2	23.2	20.3	14.8	11.5	10.6	6.6	9.3	10.0
SM	0.00009	62.2	45.4	46.9	49.2	54.5	59.5	59.9	64.8	57.7	47.5	54.1	50.0	52.0
ML	0.7608	2.3	2.8	3.6	3.4	4.5	4.5	5.7	5.1	15.4	23.8	19.7	16.7	20.0
CL	0.6809	0.3	0.0	0.0	0.7	0.0	2.5	2.2	1.5	1.5	2.5	3.3	3.7	2.0
CH	0.884	1.1	1.4	0.7	1.0	2.4	3.7	2.6	3.6	6.9	7.4	6.5	7.4	8.0
OL	0.1938	0.3	0.0	0.2	0.3	0.3	0.8	1.8	1.0	0.8	2.5	0.0	0.0	2.0
OH	0.5729	0.3	1.4	1.7	2.0	2.4	1.7	3.1	5.1	4.6	4.1	9.8	12.9	4.0

SP-SM) decrease with a constant percentage of SM class, while the fine soil classes (OL, CH, ML) increase. The soil after 16 m depth becomes a mixed soil of sand, clay, high-elastic clay, and organic matter.

Figure 10 indicates that the coarse soil (Sand) percentage was very high in the upper depths level, where it was 95% at 2 m. These percentages decrease gradually with depth, and this change in the soil became obvious after 16 m as the coarse soil percentage became 71% at 18 m and reached 64% at 26 m, while the fine soil is opposite as in coarse soil, its percentage increases with depth. It can be noticed that the coarse soil percentage drops while fine soil percentage increases at about 18 m depth, and this depth could be the contact between Dibdiba and Injana formations.

Geotechnical engineers have created charts based on experience to help designers in selecting the appropriate soil for a particular construction. These charts results are listed in Table 4. The table is used only as a guide and for making a preliminary assessment of the soil suitability for specific use (Budhu 2015). After applying the Unified Soil Classification System, the soil is evaluated depending on Table 4. In the depths between 0 and 16 m, coarse soil is dominant, with an 85–95% percentage. The coarse soil classes present are (SM, SP, and SP-SM). The fine soil percentage was about 5–15%, so when the soil for these depths is compacted and saturated, it will have a permeability of previous to semi- previous, good shearing strength, low to very low compressibility and acceptable workability as a construction material. At depths of between 16 and 26 m, the percentage of fine soil classes increases to 40%, with 60% coarse classes, and this will result in remarkable changes in soil characteristics as the permeability becomes semi-pervious to impervious, fair shearing strength, medium compressibility and fair workability as a construction material.

5 Conclusions

a. This study used the GIS software to produce geotechnical maps, which will help to prepare a database for the city and can be utilised for primary designs.

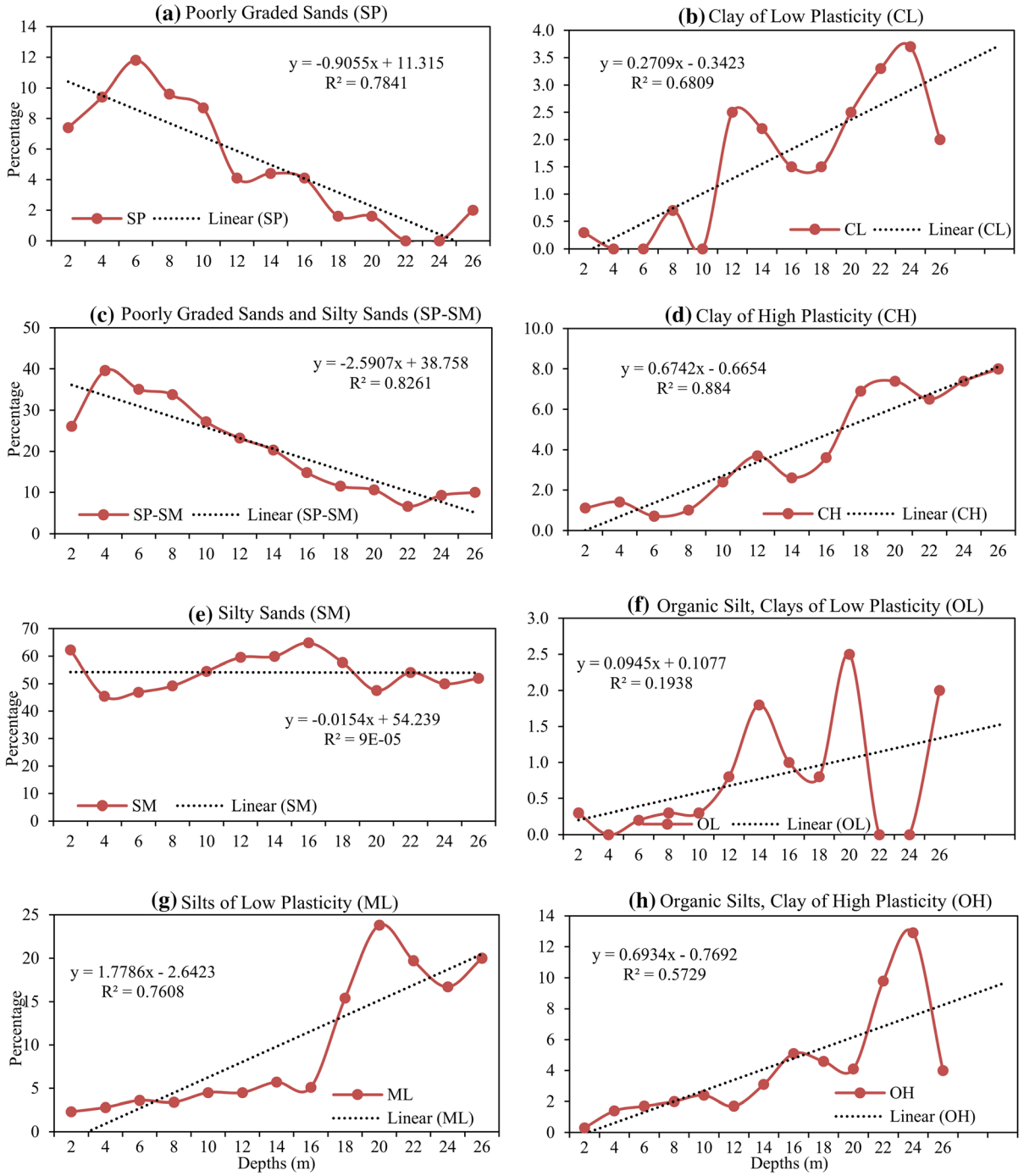

Fig. 8 Linear trend of soil classes percentage with depth

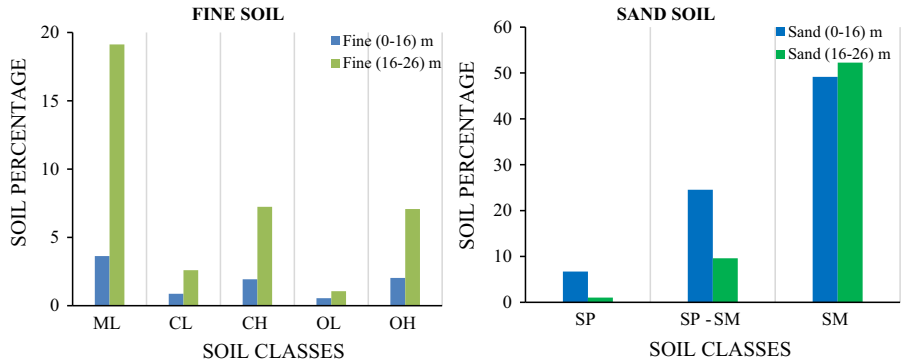

Fig. 9 Changes in the percentage of soil types before and after the depth of 16 m

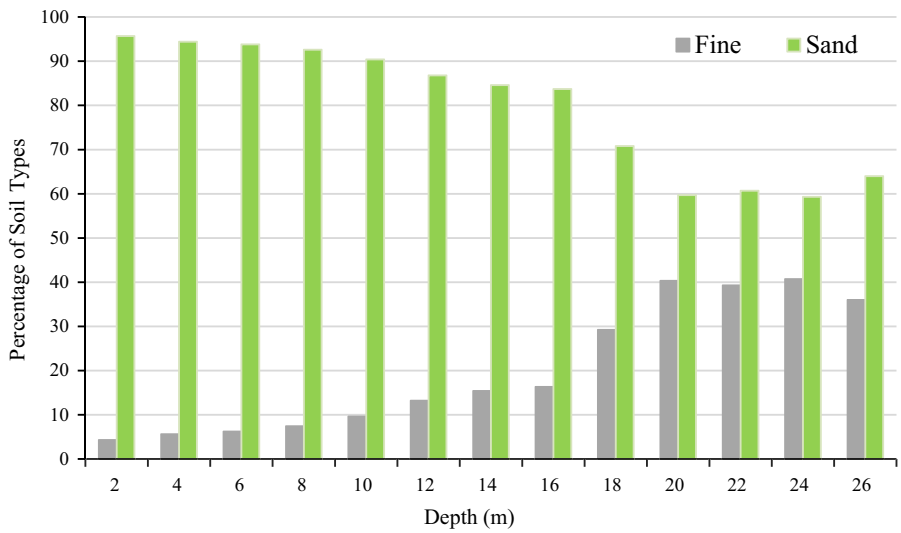

Fig. 10 Changes in soil content percentage (Sand and Fine) with depth

b. Indicator Kriging gives significant interpolated categorical (nominal) data maps for soil USCS classes.
c. The results of geotechnical maps of soil classification show that the coarse soil classes occupy most of the study area in all depths, while the fine soil appears with depth especially after the depth 6 m and in the south, middle and north of study area.
d. The final geotechnical maps are very easy to use and help save money and time. They also provide a useful database for the city.
e. The soil of An-Najaf city for depths of 0–16 m consists of the classes SP, SM, SP-SM at a percentage of 85%. Subsequently, when compacted, this soil has a permeability of pervious to semi-pervious, good shearing strength, low to very low compressibility and acceptable workability as a construction material.
f. At depths of 16–26 m, the percentage of fine soil classes increases to 40%, with 60% coarse classes, and this will result in remarkable changes in soil characteristics as the permeability became semi-pervious to impervious, fair shearing strength, medium compressibility and fair workability as a construction material.

Table 4 Engineering use chart. *Source*: after (Budhu 2015)

Group symbols	Important properties			
	Permeability when compacted	Shearing strength when compacted and saturated	Compressibility when compacted and saturated	Workability as a construction material
GW	Pervious	Excellent	Negligible	Excellent
GP	Very Pervious	Good	Negligible	Good
GM	Semipervious to impervious	Good	Negligible	Good
GC	Impervious	Good to fair	Very low	Good
SW	Previous	Excellent	Negligible	Excellent
SP	Previous	Good	Very low	Fair
SM	Semipervious to impervious	Good	Low	Fair
SC	Impervious	Good to fair	Low	Good
ML	Semipervious to impervious	Fair	Medium	Fair
CL	Impervious	Fair	Medium	Good to fair
OL	Semipervious to impervious	Poor	Medium	Fair
MH	Semipervious to impervious	Fair to poor	High	Poor
CH	Impervious	Poor	High	Poor
OH	Impervious	Poor	High	Poor
Pt	–	–	–	–

Acknowledgements Open access funding provided by Lulea University of Technology. We acknowledge the assistance of the Staff of the National Center for Construction Laboratories & Research (NCCLR)/Babylon branch for providing the data and special thanks to the head of the investigation department in NCCLR, Ms. Suhair Kamaleddin, for her help.

Appendix: Boreholes Locations' Coordinates

See Table 5.

Table 5 Location and coordinates of breholes used

No.	Code	Long.	Lat.	No.	Code	Long.	Lat.	No.	Code	Long.	Lat.
1	1001	44 20′ 56″	32 0′ 6″	156	3046	44 21′ 18″	32 0′ 41″	311	2100	44 19′ 28″	32 4′ 2″
2	2001	44 20′ 56″	32 0′ 6″	157	4046	44 21′ 20″	32 0′ 42″	312	1101	44 18′ 30″	32 2′ 30″
3	1002	44 20′ 51″	32 0′ 25″	158	5046	44 18′ 49″	31 59′ 43″	313	2101	44 18′ 30″	32 2′ 31″
4	2002	44 20′ 50″	32 0′ 25″	159	6046	44 18′ 45″	31 59′ 43″	314	3101	44 18′ 31″	32 2′ 32″
5	3002	44 20′ 49″	32 0′ 25″	160	7046	44 18′ 40″	31 59′ 43″	315	1102	44 18′ 33″	31 59′ 53″
6	1003	44 20′ 40″	32 2′ 39″	161	8046	44 18′ 37″	31 59′ 43″	316	2102	44 18′ 35″	31 59′ 51″
7	2003	44 20′ 40″	32 2′ 39″	162	9046	44 18′ 51″	31 59′ 48″	317	1103	44 16′ 59″	32 1′ 0″
8	1004	44 19′ 43″	32 0′ 15″	163	10046	44 18′ 54″	31 59′ 48″	318	2103	44 16′ 54″	32 0′ 57″
9	2004	44 19′ 42″	32 0′ 17″	164	11046	44 18′ 55″	31 59′ 44″	319	3103	44 16′ 52″	32 1′ 4″

Table 5 continued

No.	Code	Long.	Lat.	No.	Code	Long.	Lat.	No.	Code	Long.	Lat.
10	1005	44 20′ 0″	32 0′ 44″	165	12046	44 18′ 54″	31 59′ 43″	320	1104	44 23′ 33″	32 0′ 13″
11	2005	44 19′ 57″	32 0′ 47″	166	13046	44 18′ 52″	31 59′ 42″	321	2104	44 23′ 32″	32 0′ 14″
12	1006	44 19′ 13″	32 4′ 11″	167	1047	44 21′ 28″	32 0′ 42″	322	3104	44 23′ 32″	32 0′ 13″
13	2006	44 19′ 14″	32 4′ 10″	168	2047	44 21′ 29″	32 0′ 42″	323	1105	44 20′ 35″	32 1′ 37″
14	1007	44 18′ 34″	31 59′ 45″	169	3047	44 21′ 28″	32 0′ 41″	324	2105	44 20′ 37″	32 1′ 37″
15	2007	44 18′ 33″	31 59′ 44″	170	4047	44 21′ 28″	32 0′ 42″	325	1106	44 20′ 42″	31 59′ 26″
16	3007	44 18′ 33″	31 59′ 45″	171	5047	44 21′ 29″	32 0′ 41″	326	2106	44 20′ 42″	31 59′ 26″
17	1008	44 18′ 39″	31 59′ 28″	172	6047	44 21′ 29″	32 0′ 42″	327	1107	44 21′ 9″	32 0′ 29″
18	2008	44 19′ 4″	31 59′ 29″	173	1048	44 19′ 42″	32 0′ 28″	328	2107	44 21′ 9″	32 0′ 28″
19	1009	44 17′ 32″	32 0′ 25″	174	2048	44 19′ 42″	32 0′ 28″	329	1108	44 18′ 46″	32 2′ 34″
20	2009	44 17′ 36″	32 0′ 29″	175	1049	44 20′ 37″	32 0′ 28″	330	2108	44 18′ 47″	32 2′ 20″
21	3009	44 17′ 34″	32 0′ 31″	176	2049	44 20′ 36″	32 0′ 27″	331	1109	44 20′ 32″	31 59′ 4″
22	4009	44 17′ 29″	32 0′ 28″	177	3049	44 20′ 35″	32 0′ 29″	332	2109	44 20′ 29″	31 59′ 0″
23	5009	44 17′ 23″	32 0′ 30″	178	4049	44 20′ 36″	32 0′ 29″	333	1110	44 23′ 38″	32 1′ 33″
24	6009	44 17′ 29″	32 0′ 37″	179	5049	44 20′ 36″	32 0′ 28″	334	2110	44 23′ 24″	32 1′ 33″
25	7009	44 17′ 21″	32 0′ 32″	180	1050	44 20′ 47″	32 0′ 26″	335	1111	44 20′ 11″	31 59′ 21″
26	8009	44 17′ 19″	32 0′ 34″	181	2050	44 20′ 47″	32 0′ 26″	336	2111	44 20′ 10″	31 59′ 21″
27	9009	44 17′ 21″	32 0′ 37″	182	1051	44 19′ 6″	31 59′ 45″	337	1112	44 21′ 16″	32 1′ 11″
28	10009	44 17′ 15″	32 0′ 37″	183	2051	44 19′ 5″	31 59′ 45″	338	2112	44 21′ 16″	32 1′ 4″
29	1010	44 18′ 24″	32 3′ 55″	184	1052	44 19′ 1″	31 59′ 45″	339	1113	44 22′ 55″	31 58′ 35″
30	2010	44 18′ 25″	32 3′ 54″	185	2052	44 19′ 1″	31 59′ 44″	340	2113	44 22′ 54″	31 58′ 36″
31	1011	44 22′ 40″	32 1′ 4″	186	1053	44 19′ 14″	31 59′ 47″	341	3113	44 22′ 53″	31 58′ 36″
32	2011	44 22′ 44″	32 1′ 3″	187	2053	44 19′ 14″	31 59′ 47″	342	1114	44 22′ 7″	32 3′ 34″
33	3011	44 22′ 42″	32 1′ 5″	188	1054	44 19′ 0″	31 59′ 44″	343	1115	44 18′ 33″	31 59′ 40″
34	1012	44 18′ 37″	31 59′ 40″	189	2054	44 19′ 0″	31 59′ 45″	344	1116	44 22′ 32″	31 58′ 31″
35	2012	44 18′ 36″	31 59′ 40″	190	1055	44 18′ 4″	31 59′ 28″	345	2116	44 22′ 31″	31 58′ 29″
36	1013	44 19′ 53″	32 0′ 44″	191	2055	44 22′ 40″	31 58′ 14″	346	1117	44 19′ 40″	32 1′ 58″
37	2013	44 19′ 53″	32 0′ 43″	192	3055	44 22′ 30″	31 58′ 43″	347	2117	44 19′ 40″	32 1′ 58″
38	3013	44 19′ 56″	32 0′ 43″	193	4055	44 18′ 56″	31 59′ 45″	348	3117	44 19′ 40″	32 1′ 58″
39	4013	44 19′ 56″	32 0′ 44″	194	1056	44 21′ 4″	31 59′ 41″	349	4117	44 19′ 40″	32 1′ 58″
40	5013	44 19′ 54″	32 0′ 44″	195	2056	44 21′ 5″	31 59′ 43″	350	5117	44 19′ 40″	32 1′ 58″
41	6013	44 19′ 54″	32 0′ 45″	196	1057	44 20′ 21″	32 3′ 52″	351	6117	44 19′ 40″	32 1′ 58″
42	7013	44 20′ 2″	32 0′ 44″	197	2057	44 20′ 23″	32 3′ 51″	352	7117	44 19′ 40″	32 1′ 58″
43	1014	44 21′ 17″	32 0′ 27″	198	3057	44 20′ 20″	32 3′ 52″	353	8117	44 19′ 40″	32 1′ 58″
44	2014	44 21′ 18″	32 0′ 26″	199	4057	44 20′ 22″	32 3′ 52″	354	1118	44 20′ 14″	32 2′ 51″
45	1015	44 21′ 29″	32 0′ 48″	200	1058	44 20′ 40″	32 0′ 28″	355	2118	44 20′ 14″	32 2′ 50″
46	2015	44 21′ 14″	32 0′ 57″	201	2058	44 20′ 41″	32 0′ 28″	356	1119	44 20′ 57″	32 0′ 2″
47	1016	44 21′ 27″	32 1′ 4″	202	3058	44 20′ 43″	32 0′ 29″	357	2119	44 20′ 58″	32 0′ 1″
48	2016	44 21′ 30″	32 0′ 43″	203	4058	44 20′ 44″	32 0′ 29″	358	1120	44 22′ 13″	32 0′ 1″
49	1017	44 23′ 29″	31 59′ 34″	204	5058	44 20′ 42″	32 0′ 27″	359	2120	44 22′ 14″	32 0′ 1″
50	2017	44 23′ 43″	31 59′ 30″	205	6058	44 20′ 43″	32 0′ 28″	360	1121	44 20′ 21″	32 0′ 19″
51	3017	44 24′ 2″	31 59′ 26″	206	7058	44 20′ 41″	32 0′ 26″	361	2121	44 20′ 22″	32 0′ 19″
52	4017	44 24′ 18″	31 59′ 23″	207	8058	44 20′ 43″	32 0′ 27″	362	1122	44 18′ 59″	31 59′ 43″
53	1018	44 18′ 46″	31 59′ 40″	208	9058	44 20′ 45″	32 0′ 28″	363	2122	44 18′ 57″	31 59′ 28″
54	2018	44 18′ 46″	31 59′ 40″	209	10058	44 20′ 42″	32 0′ 26″	364	1123	44 18′ 44″	32 6′ 4″

Table 5 continued

No.	Code	Long.	Lat.	No.	Code	Long.	Lat.	No.	Code	Long.	Lat.
55	1019	44 18′ 47″	31 59′ 46″	210	12058	44 20′ 46″	32 0′ 28″	365	2123	44 18′ 36″	32 7′ 14″
56	2019	44 18′ 48″	31 59′ 43″	211	14058	44 20′ 43″	32 0′ 25″	366	1124	44 18′ 6″	32 11′ 28″
57	3019	44 18′ 41″	31 59′ 44″	212	1059	44 18′ 36″	31 59′ 24″	367	2124	44 19′ 50″	32 0′ 5″
58	1020	44 19′ 22″	31 59′ 49″	213	2059	44 18′ 36″	31 59′ 28″	368	1125	44 19′ 31″	32 0′ 53″
59	2020	44 19′ 22″	31 59′ 49″	214	1060	44 20′ 12″	32 2′ 43″	369	2125	44 19′ 32″	32 0′ 56″
60	1021	44 18′ 38″	31 59′ 41″	215	2060	44 20′ 8″	32 2′ 43″	370	1126	44 20′ 20″	31 59′ 51″
61	2021	44 18′ 38″	31 59′ 41″	216	1061	44 18′ 59″	31 59′ 44″	371	2126	44 20′ 21″	31 59′ 51″
62	1022	44 21′ 6″	31 59′ 26″	217	2061	44 18′ 58″	31 59′ 44″	372	1127	44 20′ 32″	32 1′ 34″
63	2022	44 21′ 6″	31 59′ 29″	218	1062	44 21′ 11″	32 1′ 11″	373	2127	44 20′ 32″	32 1′ 33″
64	1023	44 22′ 48″	31 59′ 28″	219	2062	44 21′ 14″	32 1′ 7″	374	1128	44 18′ 57″	31 59′ 30″
65	2023	44 23′ 49″	31 59′ 28″	220	1063	44 19′ 4″	31 59′ 45″	375	1129	44 19′ 16″	31 59′ 19″
66	3023	44 24′ 15″	31 58′ 51″	221	2063	44 19′ 3″	31 59′ 44″	376	2129	44 19′ 17″	31 59′ 18″
67	4023	44 23′ 28″	31 59′ 56″	222	1064	44 17′ 32″	32 8′ 13″	377	1130	44 19′ 18″	32 3′ 56″
68	5023	44 23′ 53″	31 59′ 29″	223	2064	44 13′ 11″	32 8′ 17″	378	2130	44 19′ 18″	32 3′ 55″
69	6023	44 23′ 57″	31 59′ 28″	224	1065	44 17′ 54″	32 7′ 43″	379	1131	44 19′ 51″	31 59′ 6″
70	7023	44 23′ 51″	31 59′ 29″	225	1066	44 18′ 57″	31 59′ 44″	380	2131	44 19′ 50″	31 59′ 5″
71	8023	44 23′ 51″	31 59′ 29″	226	2066	44 18′ 58″	31 59′ 44″	381	1132	44 21′ 41″	32 0′ 41″
72	9023	44 23′ 50″	31 59′ 29″	227	1067	44 20′ 59″	32 2′ 44″	382	2132	44 21′ 40″	32 0′ 40″
73	10023	44 23′ 55″	31 59′ 28″	228	2067	44 21′ 0″	32 2′ 43″	383	1133	44 19′ 11″	31 59′ 56″
74	11023	44 23′ 54″	31 59′ 29″	229	1068	44 21′ 31″	32 1′ 16″	384	2133	44 17′ 28″	32 0′ 35″
75	12023	44 23′ 22″	31 59′ 41″	230	2068	44 21′ 33″	32 1′ 17″	385	3133	44 17′ 29″	32 0′ 31″
76	1024	44 21′ 3″	32 0′ 40″	231	1069	44 19′ 5″	31 59′ 43″	386	1134	44 19′ 6″	31 59′ 50″
77	2024	44 21′ 3″	32 0′ 39″	232	2069	44 19′ 5″	31 59′ 43″	387	2134	44 19′ 6″	31 59′ 50″
78	1025	44 18′ 33″	31 59′ 49″	233	1070	44 19′ 10″	31 59′ 38″	388	1135	44 4′ 34″	31 6′ 11″
79	2025	44 18′ 33″	31 59′ 49″	234	2070	44 19′ 10″	31 59′ 39″	389	2135	44 4′ 10″	31 6′ 47″
80	3025	44 18′ 32″	31 59′ 48″	235	1071	44 19′ 2″	31 59′ 44″	390	3135	44 3′ 7″	31 11′ 20″
81	4025	44 18′ 32″	31 59′ 48″	236	2071	44 19′ 3″	31 59′ 45″	391	1136	44 18′ 42″	31 59′ 51″
82	1026	44 16′ 46″	32 1′ 12″	237	1072	44 19′ 9″	31 59′ 38″	392	2136	44 18′ 42″	31 59′ 51″
83	2026	44 16′ 41″	32 1′ 12″	238	2072	44 19′ 10″	31 59′ 37″	393	1137	44 18′ 47″	32 3′ 12″
84	1027	44 19′ 52″	31 59′ 59″	239	1073	44 18′ 40″	31 59′ 41″	394	2137	44 18′ 47″	32 3′ 11″
85	2027	44 19′ 52″	31 59′ 59″	240	2073	44 18′ 40″	31 59′ 40″	395	1138	44 21′ 12″	32 1′ 55″
86	1028	44 19′ 11″	31 59′ 42″	241	1074	44 19′ 8″	31 59′ 39″	396	2138	44 21′ 12″	32 1′ 54″
87	2028	44 19′ 11″	31 59′ 42″	242	2074	44 19′ 8″	31 59′ 40″	397	1139	44 20′ 57″	32 1′ 7″
88	1029	44 19′ 56″	32 0′ 2″	243	1075	44 19′ 9″	31 59′ 39″	398	2139	44 20′ 56″	32 1′ 8″
89	2029	44 19′ 54″	32 0′ 2″	244	2075	44 19′ 9″	31 59′ 39″	399	1140	44 18′ 36″	31 59′ 50″
90	3029	44 19′ 56″	32 0′ 3″	245	1076	44 19′ 9″	31 59′ 40″	400	2140	44 18′ 36″	31 59′ 49″
91	4029	44 19′ 56″	31 59′ 58″	246	2076	44 19′ 9″	31 59′ 40″	401	1141	44 18′ 35″	31 59′ 49″
92	5029	44 19′ 57″	31 59′ 59″	247	1077	44 19′ 3″	31 59′ 46″	402	2141	44 18′ 35″	31 59′ 49″
93	6029	44 19′ 59″	32 0′ 2″	248	2077	44 19′ 4″	31 59′ 46″	403	1142	44 18′ 47″	32 3′ 12″
94	7029	44 19′ 59″	32 0′ 0″	249	1078	44 19′ 9″	31 59′ 41″	404	2142	44 18′ 47″	32 3′ 11″
95	1030	44 19′ 48″	32 0′ 4″	250	2078	44 19′ 9″	31 59′ 41″	405	1143	44 20′ 53″	32 2′ 14″
96	2030	44 19′ 51″	32 0′ 2″	251	1079	44 21′ 12″	32 0′ 29″	406	2143	44 20′ 52″	32 2′ 14″
97	3030	44 19′ 51″	32 0′ 4″	252	2079	44 21′ 11″	32 0′ 29″	407	1144	44 19′ 2″	31 59′ 52″
98	4030	44 19′ 50″	32 0′ 5″	253	1080	44 21′ 12″	32 0′ 54″	408	2144	44 19′ 2″	31 59′ 51″
99	1031	44 21′ 22″	31 58′ 42″	254	2080	44 21′ 13″	32 0′ 52″	409	1145	44 18′ 51″	32 3′ 13″

Table 5 continued

No.	Code	Long.	Lat.	No.	Code	Long.	Lat.	No.	Code	Long.	Lat.
100	2031	44 21′ 16″	31 58′ 46″	255	1081	44 19′ 0″	31 59′ 46″	410	2145	44 18′ 51″	32 3′ 12″
101	3031	44 21′ 10″	31 58′ 47″	256	2081	44 18′ 59″	31 59′ 46″	411	1146	44 18′ 46″	31 59′ 49″
102	4031	44 21′ 20″	31 58′ 45″	257	1082	44 19′ 5″	31 59′ 46″	412	2146	44 18′ 46″	31 59′ 50″
103	5031	44 21′ 13″	31 58′ 48″	258	2082	44 19′ 5″	31 59′ 46″	413	1147	44 19′ 56″	32 1′ 49″
104	6031	44 21′ 26″	31 58′ 46″	259	1083	44 21′ 13″	32 0′ 35″	414	2147	44 19′ 56″	32 1′ 51″
105	7031	44 21′ 17″	31 58′ 48″	260	2083	44 21′ 12″	32 0′ 36″	415	1148	44 18′ 59″	32 3′ 58″
106	8031	44 21′ 12″	31 58′ 51″	261	3083	44 21′ 12″	32 0′ 36″	416	2148	44 18′ 58″	32 3′ 40″
107	1032	44 21′ 28″	32 0′ 42″	262	4083	44 21′ 12″	32 0′ 36″	417	3148	44 19′ 0″	32 3′ 46″
108	2032	44 21′ 28″	32 0′ 42″	263	1084	44 18′ 58″	31 59′ 46″	418	1149	44 19′ 36″	32 5′ 14″
109	3032	44 21′ 29″	32 0′ 41″	264	2084	44 18′ 57″	31 59′ 46″	419	2149	44 19′ 42″	32 5′ 13″
110	4032	44 21′ 29″	32 0′ 42″	265	1085	44 19′ 1″	31 59′ 46″	420	3149	44 19′ 39″	32 5′ 14″
111	1033	44 20′ 3″	31 59′ 37″	266	2085	44 19′ 0″	31 59′ 46″	421	1150	44 19′ 36″	32 3′ 19″
112	2033	44 20′ 3″	31 59′ 37″	267	1086	44 18′ 38″	31 52′ 54″	422	2150	44 19′ 37″	32 3′ 18″
113	1034	44 22′ 50″	31 58′ 36″	268	2086	44 18′ 38″	31 21′ 53″	423	3150	44 19′ 35″	32 3′ 18″
114	2034	44 22′ 52″	31 58′ 40″	269	1087	44 19′ 0″	31 59′ 46″	424	1151	44 21′ 44″	32 2′ 24″
115	3034	44 22′ 53″	31 58′ 37″	270	2087	44 18′ 59″	31 59′ 46″	425	2151	44 21′ 42″	32 2′ 23″
116	4034	44 22′ 54″	31 58′ 36″	271	1088	44 18′ 38″	31 59′ 40″	426	3151	44 21′ 45″	32 2′ 22″
117	5034	44 22′ 57″	31 58′ 36″	272	2088	44 18′ 38″	31 59′ 40″	427	4151	44 21′ 47″	32 2′ 23″
118	6034	44 22′ 55″	31 58′ 33″	273	1089	44 18′ 40″	31 59′ 40″	428	5151	44 21′ 45″	32 2′ 26″
119	1035	44 20′ 15″	32 2′ 19″	274	2089	44 18′ 43″	31 59′ 40″	429	6151	44 21′ 43″	32 2′ 26″
120	2035	44 20′ 14″	32 2′ 19″	275	1090	44 21′ 48″	32 2′ 15″	430	1152	44 21′ 8″	32 2′ 45″
121	3035	44 20′ 15″	32 2′ 19″	276	2090	44 21′ 48″	32 2′ 14″	431	2152	44 21′ 0″	32 1′ 15″
122	1036	44 18′ 29″	31 59′ 41″	277	1091	44 21′ 20″	32 0′ 40″	432	3152	44 21′ 28″	32 1′ 16″
123	2036	44 18′ 29″	31 59′ 39″	278	2091	44 21′ 19″	32 0′ 42″	433	4152	44 19′ 5″	31 59′ 44″
124	3036	44 18′ 28″	31 59′ 40″	279	3091	44 21′ 20″	32 0′ 42″	434	5152	44 19′ 4″	31 59′ 42″
125	4036	44 18′ 28″	31 59′ 41″	280	4091	44 21′ 18″	32 0′ 42″	435	1153	44 19′ 8″	31 59′ 38″
126	5036	44 18′ 27″	31 59′ 41″	281	5091	44 18′ 48″	31 59′ 42″	436	2153	44 19′ 11″	31 58′ 52″
127	1037	44 18′ 47″	31 59′ 42″	282	6091	44 18′ 36″	31 59′ 29″	437	1154	44 23′ 37″	32 1′ 36″
128	2037	44 18′ 48″	31 59′ 42″	283	7091	44 18′ 40″	31 59′ 54″	438	2154	44 23′ 36″	32 1′ 37″
129	1038	44 18′ 36″	31 59′ 41″	284	8091	44 18′ 39″	31 59′ 45″	439	1155	44 22′ 48″	31 58′ 35″
130	2038	44 18′ 36″	31 59′ 41″	285	9091	44 18′ 50″	31 59′ 49″	440	2155	44 22′ 48″	31 58′ 38″
131	1039	44 18′ 43″	31 59′ 42″	286	1092	44 19′ 52″	31 59′ 58″	441	3155	44 22′ 51″	31 58′ 39″
132	2039	44 18′ 44″	31 59′ 41″	287	2092	44 19′ 52″	31 59′ 58″	442	4155	44 22′ 52″	31 58′ 37″
133	1040	44 18′ 57″	32 3′ 42″	288	3092	44 19′ 52″	31 59′ 58″	443	1156	44 18′ 50″	32 2′ 24″
134	2040	44 18′ 59″	32 3′ 42″	289	1093	44 18′ 54″	31 59′ 54″	444	2156	44 18′ 49″	32 2′ 23″
135	3040	44 19′ 0″	32 3′ 43″	290	2093	44 18′ 54″	31 59′ 54″	445	1157	44 18′ 43″	32 1′ 30″
136	4040	44 18′ 59″	32 3′ 43″	291	1094	44 21′ 48″	32 0′ 43″	446	2157	44 18′ 43″	32 1′ 32″
137	1041	44 21′ 19″	32 0′ 41″	292	2094	44 21′ 40″	32 1′ 11″	447	1158	44 20′ 0″	32 0′ 5″
138	2041	44 21′ 20″	32 0′ 41″	293	1095	44 18′ 42″	32 2′ 17″	448	2158	44 19′ 59″	32 0′ 5″
139	3041	44 21′ 18″	32 0′ 41″	294	2095	44 18′ 43″	32 2′ 17″	449	1159	44 19′ 57″	31 58′ 56″
140	4041	44 21′ 20″	32 0′ 42″	295	1096	44 18′ 57″	31 59′ 48″	450	2159	44 19′ 57″	31 58′ 56″
141	1042	44 19′ 31″	32 3′ 44″	296	2096	44 18′ 58″	31 59′ 48″	451	1160	44 22′ 3″	32 0′ 36″
142	1043	44 21′ 12″	32 1′ 59″	297	3096	44 18′ 57″	31 59′ 48″	452	2160	44 22′ 2″	32 0′ 37″
143	2043	44 21′ 13″	32 2′ 0″	298	4096	44 18′ 57″	31 59′ 49″	453	1161	44 20′ 14″	32 45′ 28″
144	3043	44 21′ 13″	32 1′ 59″	299	1097	44 18′ 40″	31 59′ 53″	454	2161	44 20′ 17″	32 33′ 1″

Table 5 continued

No.	Code	Long.	Lat.	No.	Code	Long.	Lat.	No.	Code	Long.	Lat.
145	1044	44 20′ 18″	32 3′ 59″	300	2097	44 18′ 42″	31 59′ 54″	455	3161	44 20′ 19″	32 36′ 58″
146	2044	44 20′ 16″	32 4′ 0″	301	3097	44 18′ 41″	31 59′ 54″	456	4161	44 20′ 16″	32 23′ 14″
147	1045	44 18′ 47″	32 0′ 29″	302	1098	44 22′ 18″	31 59′ 37″	457	1162	44 22′ 17″	32 0′ 3″
148	2045	44 18′ 52″	32 0′ 37″	303	2098	44 22′ 18″	31 59′ 38″	458	2162	44 22′ 16″	32 0′ 4″
149	3045	44 19′ 1″	32 0′ 32″	304	3098	44 22′ 17″	31 59′ 38″	459	3162	44 22′ 17″	32 0′ 4″
150	4045	44 18′ 34″	32 0′ 34″	305	1099	44 21′ 28″	32 0′ 41″	460	4162	44 22′ 17″	32 0′ 4″
151	5045	44 18′ 38″	32 0′ 37″	306	2099	44 21′ 4″	32 0′ 41″	461	1163	44 20′ 3″	32 2′ 32″
152	6045	44 18′ 41″	32 0′ 37″	307	3099	44 21′ 28″	32 0′ 41″	462	2163	44 20′ 3″	32 2′ 32″
153	7045	44 18′ 37″	32 0′ 41″	308	4099	44 21′ 35″	32 0′ 42″	463	1164	44 21′ 29″	32 0′ 42″
154	1046	44 21′ 19″	32 0′ 41″	309	5099	44 19′ 3″	31 59′ 42″	464	2164	44 21′ 28″	32 0′ 41″
155	2046	44 21′ 20″	32 0′ 41″	310	1100	44 19′ 26″	32 4′ 2″				

References

Al-Baghdadi NH (2016) Geotechnical mapping of An-Najaf City, Iraq. J Univ Babylon 24(4):962–979

Ali TS, Fakhraldin MK (2016) Soil parameters analysis of Al-Najaf City in Iraq: case study. J Geotech Eng 3(1):56–62

Al-Maliki LAJ, Al-Mamoori SK, El-Tawel K, Hussain HM, Al-Ansari N, Jawad Al Ali M (2018) Bearing capacity map for An-Najaf and Kufa Cities using GIS. Engineering 10(05):262–269. https://doi.org/10.4236/eng.2018.105018

Al-Mamoori SK (2017) Gypsum content horizontal and vertical distribution of An-Najaf and Al-Kufa Cities' soil by using GIS. Basrah J Eng Sci 17(1):48–60

Al-Mamoori SK, Al-Maliki LA, Hussain HM, Al-Ali MJ (2018) Distribution of sulfate content and organic matter in An-Najaf and Al-Kufa Cities'soil using GIS. Kufa J Eng 9(3):92–111

Al-Mamoori SK, Al-Maliki LAJ, El-Tawel K, Hussain HM, Al-Ansari N, Al Ali MJ (2019) Chloride, calcium carbonate and total soluble salts contents distribution for An-Najaf and Al-Kufa Cities' soil by using GIS. Geotech Geol Eng 37(3):2207–2225

Al-Mubarak M, Amin R (1983) Report on the regional geological mapping of the eastern part of the Western Desert and western part of the Southern Desert, Library of the geological survey of Iraq (GEOSURV), Internal report number (1380), Baghdad, Iraq

Al-Shakerchy YJ, Al-Khuzaie MA (2011) The geotechnical maps for the soil of the governorates of Baghdad, Diyala, Wasit and Babylon. J Eng 17(3):87–104

ASTM (2000) Standard classification of soils for engineering purposes (unified soil classification system), vol 4

Barwary A, Slewa N (1994) The geology of Al-Najaf quadrangle NH-38-2, scale 1: 250 000, Library of the geological survey of Iraq (GEOSURV), Internal report, Baghdad, Iraq

Barwary A, Slewa N (1995) The geology of Karbala quadrangle (NH-38-6), scale 1: 250 000. GEOSURV Int Rep 2318

Beg AAF, Al-Sulttani AH (2020) Spatial assessment of drought conditions over Iraq using the standardized precipitation index (SPI) and GIS techniques. In: Al-Quraishi AMF, Negm A (eds) Environmental remote sensing and GIS in Iraq. Springer, Switzerland, pp 447–462. https://doi.org/10.1007/978-3-030-21344-2

Bhunia GS, Shit PK, Maiti R (2018) Comparison of GIS-based interpolation methods for spatial distribution of soil organic carbon (SOC). J Saudi Soc Agric Sci 17(2):114–126

Buday T (1980) The regional geology of Iraq. Stratigraphy and paleogeography, vol 1. Baghdad, GEOSURV, p 445

Budhu M (2015) Soil mechanics fundamentals. Wiley, New York

Childs C (2004) Interpolating surfaces in ArcGIS spatial analyst. ArcUser 3235:569

Dai F, Lee C, Zhang X (2001) GIS-based geo-environmental evaluation for urban land-use planning: a case study. Eng Geol 61(4):257–271

Das BM (2013) Advanced soil mechanics. CRC Press, Boca Raton

Das BM, Sobhan K (2013) Principles of geotechnical engineering. Cengage learning

Jassim SZ, Goff JC (2006) Geology of Iraq. Dolin, Prague and Moravian Museum, Brno

LIU F-c, Peng J, C-y ZHANG (2012) A non-parametric indicator Kriging method for generating coastal sediment type map. Mar Sci Bull 14(1):57–67

Mail AASM, Somorowska U, Al-Sulttani AH (2016) Seasonal and inter-annual variation of precipitation in Iraq over the period 1992–2010. Prace i Studia Geograficzne 61(3):71–84

Mendes RM, Lorandi R (2006) Indicator kriging geostatistical methodology applied to geotechnics project planning. IAEG2006 Pap 527:1–12

NCCLR (2016) An-Najaf soils investigation reports. National Center for Construction Laboratories & Research (NCCLR), Governorate of Babylon, Babylon

Reale C, Gavin K, Librić L, Jurić-Kaćunić D (2018) Automatic classification of fine-grained soils using CPT measurements and artificial neural networks. Adv Eng Inform 36:207–215

Reese LC, Isenhower WM, Wang S-T (2006) Analysis and design of shallow and deep foundations. Wiley, New York
Robertson P (2016) Cone penetration test (CPT)-based soil behaviour type (SBT) classification system—an update. Can Geotech J 53(12):1910–1927
Zandi S, Ghobakhlou A, Sallis P (2011) Evaluation of spatial interpolation techniques for mapping soil pH. In: Paper presented at the 19th international congress on modelling and simulation, Perth, Australia, December 2011